The following manuscript was accepted for publication in Pharmaceutical Sciences. It is assigned to an issue after technical editing, formatting for publication and author proofing.
Citation: Martihandini N, Surini S, Bahtiar A. Andrographolide-loaded ethosomal gel for transdermal application: Formulation and in vitro penetration study. Pharm Sci. 2021, doi:10.34172/PS.2021.76

Andrographolide-loaded ethosomal gel for transdermal application: Formulation and *in vitro* penetration study

Nooryza Martihandini[1], Silvia Surini[1,*], Anton Bahtiar[2]

[1]Laboratory of Pharmaceutics and Pharmaceutical Technology Development, Faculty of Pharmacy, Universitas Indonesia, Depok, West Java, 16424, Indonesia.

[2]Laboratory of Pharmacology and Toxicology, Faculty of Pharmacy, Universitas Indonesia, Depok, West Java, 16424, Indonesia

Running title: Andrographolide ethosomal gel

[*]**Corresponding author:** Silvia Surini, Laboratory of Pharmaceutics and Pharmaceutical Technology Development, Faculty of Pharmacy, Universitas Indonesia, Depok, West Java, 16424, Indonesia, Phone No: +62-21-7270031, Fax No: +62-21-7863433, Email: silvia@farmasi.ui.ac.id

Accepted Manuscript

Abstract

Background: Andrographolide is a phytoconstituent with anti-inflammatory activity, however, the compound's poor oral bioavailability has hindered its effective formulation for oral administration. This study, therefore, aims to develop an ethosome for improving andrographolide penetration through the transdermal delivery system.

Methods: This study developed 3 ethosome formulas with different andrographolide-phospholipid weight ratios (1:8, 1:9; 1:10), using the thin-layer dispersion-sonication method. Subsequently, the ethosomes were evaluated for particle size, polydispersity index, zeta potential, morphology, as well as entrapment efficiency, and incorporated into a gel dosage form. Subsequently, an *in vitro* penetration study was performed using Franz diffusion cells for 24 hours and the stability of the gels at 5 ± 2°C, 30 ± 2°C, and 40 ± 2°C, were studied for 3 months.

Results: The results showed the optimal formula was E2, a 1:9 weight ratio formula of andrographolide and phospholipid. Based on the transmission electron micrograph, E2 possessed unilamellar, as well as spherical-shaped vesicles, and exhibited superior characteristics for transdermal delivery, with a particle size of 89.95 ± 0.75 nm, polydispersity index of 0.254 ± 0.020, a zeta potential of -39.3 ± 0.82 mV, and entrapment efficiency of 97.89 ± 0.02%. Furthermore, the cumulative andrographolide penetration and transdermal flux for the ethosomal gel of E2 (EG2) were 129.25 ± 4.66 μg/cm^2 and 5.16 ± 0.10 μg/cm^2/hours, respectively. All the ethosomal gel formulations exhibited improved penetration enhancement of andrographolide, compared to the nonethosomal formulations. Also, the andrographolide levels in the ethosomal and nonethosomal gels after 3 months ranged from 98.13 to 104.19%, 97.93 to 104.01%, and 97.23 to 102.26% at storage temperatures of 5 ± 2°C, 30 ± 2°C/RH 65% ± 5%, and 40 ± 2°C/RH 75% ± 5%, respectively.

Accepted Manuscript

Conclusion: This study concluded that encapsulation into ethosome enhances andrographolide delivery through the skin.

Keywords: Andrographolide, ethosome, penetration study, transdermal, and vesicle.

Introduction

Andrographolide, a labdane diterpenoid, is the major active constituent of *Andrographis paniculata* (Burm.f) Wall ex Nees and exhibits therapeutic activity, including activity against rheumatoid arthritis and other chronic inflammatory diseases.[1,2,3] A study by Li *et al*.,[4] showed oral suspension of andrographolide reduced the arthritis severity and joint damage in mice with collagen-induced arthritis. The anti-inflammatory activity of this compound has also been proven by the antiproliferation and pro-apoptotic effects on rheumatoid arthritis fibroblast-like synoviocyte cells (RAFLS).[5]

Andrographolide has low oral bioavailability (1.19 %) mainly due to the compound's rapid metabolism in the duodenum and jejunum, forming hydrophilic and impermeable sulfate metabolites.[6,7] This low oral bioavailability is also caused by other factors, including poor water solubility (3.29 ± 0.73 µg / mL) and the presence of efflux transporters that tend to pump andrographolide back into the gut lumen.[7,8]

Transdermal drug delivery is an alternative strategy developed to improve andrographolide bioavailability by avoiding the hepatic first-pass metabolism, drug degradation, and efflux pumps in the digestive tract.[9,10] This route also reduces patient discomfort by eliminating the need for oral administration, considering the bitter taste of andrographolide. However, this method is also constrained by limited bioavailability due to the stratum corneum which is the major barrier in the drug penetration through the skin.[11]

For this reason, lipid vesicles, for instance, ethosomes, have been used in transdermal drug delivery. Ethosomes are more elastic, as well as flexible, compared to liposomes, and

Accepted Manuscript

therefore, enable drugs to penetrate the skin into the systemic circulation more easily.[12,13] The high alcohol content of the ethosome tends to disorganize and alter the permeability of the stratum corneum's lipid bilayer structure, and consequently, enhance transdermal drug penetration.[14,15] This study, then, aims to formulate andrographolide into ethosome vesicles to improve skin permeation.

Materials and Methods

Materials

Andrographolide was purchased from Sunrise Nutrachem Group Co. (Qingdao, China), while the reference standard of andrographolide was procured from Sigma Aldrich, Singapore. Furthermore, a gift sample of Phospholipon 90 G was obtained from Lipoid (Nattermannallee, Germany), while laboratory-grade ethanol, methanol, propylene glycol, potassium hydrogen phosphate, sodium hydroxide were purchased from Merck (Darmstadt, Germany). *Sprague Dawley* rats were also obtained from Bogor Agricultural University (Bogor, Indonesia).

Methods

Formulation of andrographolide-loaded ethosome

Table 1 shows the composition of the andrographolide-loaded ethosomes formulated using three different andrographolide-phospholipid weight ratios (1:8; 1:9; 1:10), as well as a hydration medium comprising ethanol (20%), propylene glycol (5%), and phosphate buffer pH 7.4 (75%).

The ethosomal suspension was prepared using the thin-layer dispersion method followed by sonication.[16] For this preparation, andrographolide and phospholipon 90G were dissolved in methanol inside a round-bottom flask, and a thin lipid film was formed by removing the organic solvent using a rotary evaporator Buchi V-100 (Buchi, Switzerland) under vacuum at

Accepted Manuscript

54°C and 50-150 rpm. Subsequently, the flask was streamed with nitrogen and stored overnight at 4°C to remove any traces of solvent. The thin lipid film on the wall of the flask was then hydrated at 40°C for 1 hour using 30 mL of hydroethanolic solution which was a 20:5:75 ratio mixture of ethanol-propylene glycol-phosphate buffer pH 7.4. This was followed by subjecting the ethosome to sonication for two minutes using a probe sonicator Qsonica CL-334 (Cole Parmer, USA) at 20% amplitude, to reduce the vesicle size.

Characterization of andrographolide-loaded ethosome

Vesicle size distribution and zeta potential measurement

The ethosomes obtained were diluted in distilled water, then the particle size and zeta potential were evaluated using a computerized particle size analyzer (PSA) Zetasizer ZS90 (Malvern, UK). All the formulas were analyzed in triplicates at a scattering angle of 90°.[17,18]

Morphology

The morphology of andrographolide-loaded ethosomes was visualized using Transmission Electron Microscopy (TEM) FEI Tecnai G2 20 S-Twin with LaB_6 filament operating at 200 kV acceleration voltage (Thermo Fisher Scientific, USA). This was performed by placing diluted ethosome onto a carbon-coated copper grid and leaving the grid to dry before placing it on a slide and conducting a TEM evaluation.

Determination of entrapment efficiency

The ethosomes' entrapment efficiency was evaluated using the centrifugation indirect method, where the ethosomes were centrifuged at 14,000 rpm and 4°C, for 1 hour. Subsequently, the supernatant containing free (unentrapped) andrographolide was collected, diluted with methanol, and subjected to HPLC analysis to determine the drug concentration. The entrapment efficiency of andrographolide in the ethosome was then calculated using the following formula.[16,19]

Accepted Manuscript

$$\text{Entrapment efficiency (\%)} = \frac{\text{Total drug} - \text{Free drug}}{\text{Total drug}} \text{ x } 100$$

Formulation and evaluation of andrographolide-loaded ethosomal gel

Each andrographolide-loaded ethosome was incorporated into a gel in a dose of about 10 mg andrographolide/gram gel. Meanwhile, andrographolide gel was also formulated without ethosome to serve as a comparison. Table 2 shows the composition of the gels which were formulated using HPMC with a concentration of 1.5% (w/w) as a gelling agent. HPMC was dispersed in water at 70 - 90°C for 10 minutes and stirred until a homogeneous dispersion was formed. Meanwhile, methylparaben and propylparaben were dissolved in propylene glycol and mixed with HPMC dispersion to form a homogeneous gel base. Subsequently, andrographolide-loaded ethosome was added to the gel base in the homogenizer and stirred at 100 rpm for 15 minutes. The organoleptic, homogeneity, pH value, viscosity, and rheology properties of the gels obtained were then evaluated.

In vitro penetration study

The *in vitro* penetration of the ethosomal and nonethosomal gels through the abdominal skin of male *Sprague-Dawley* rats were evaluated using the Franz diffusion cells with a permeation area of 1.77 cm^2 and receptor cell volume of 15 mL. The receptor compartment medium comprised phosphate buffer pH 7.4 and methanol (90:10) maintained at 37 ± 0.5°C and constantly stirred by a magnetic stirrer at 300 rpm throughout the experiment. For this evaluation, the rat skin was placed in a Franz diffusion cell with the stratum corneum positioned upside toward the donor compartment and the dermis downside against the receptor compartment. Subsequently, a sample of gel equivalent to 10 mg andrographolide was applied to the skin surface and each experiment was performed in triplicate. Samples of 1.0 mL were collected from the receptor compartment through the sampling port at various time intervals and analyzed by HPLC to determine the concentration of andrographolide. The

Accepted Manuscript

graph of the cumulative amount of andrographolide penetrated against time was then plotted and the steady-state flux was calculated from the slope of the linear portion.

Stability study

Ethosomes and gel preparations were sealed and stored for 3 months at 5°C ± 2°C, 30 ± 2°C/RH 65% ± 5%, and 40 ± 2°C/RH 75% ± 5%. Subsequently, the ethosome and gel samples were withdrawn each month at a predetermined time and the ethosomes were analyzed for vesicle size and polydispersity index, while the ethosomal and nonethosomal gels were subjected to organoleptic, homogeneity, pH, viscosity, and the andrographolide content evaluations.

Chromatographic condition for determination of andrographolide content

Andrographolide was analyzed using an HPLC instrument (Shimadzu, Japan) equipped with a UV detector set at 225 nm. Separation was performed using the Zorbax Eclipse Plus C18 column (250 x 4.6 mm, 5 µm particle), and the mobile phase composition was methanol-water (52:48, v/v) at an isocratic flow rate of 0.8 mL/min.[20]

Statistical Analysis

All results were presented as mean ± standard deviation. The statistically significant differences in the result of *in vitro* penetration study was determined by a T test performed with Microsoft Office Excel, using a P value < 0.05.

Results

Characterization of andrographolide-loaded ethosome

<u>Vesicle size distribution and zeta potential measurement</u>

The ethosome vesicle sizes were determined using dynamic light scattering (DLS) and expressed as the mean hydrodynamic diameter (Z-average). Figure 1 shows the vesicle size distribution of the ethosomes obtained, while Table 3 shows a summary of the vesicle sizes

Accepted Manuscript

and zeta potentials of the andrographolide-loaded ethosomes. The results showed the ethosomes ranged from 87.40 to 100.25 nm in size, with E3 having the largest vesicle size. Furthermore, the PDI of all the formulas was below 0.3. Using the same tool, the values of zeta potential were also determined in triplicate. Table 3 shows the zeta potentials of E1, E2, and E3 ethosomes were -29.67 ± 1.03 mV, -39.30 ± 0.82 mV, and -33.43 ± 0.97 mV, respectively.

Morphology

The ethosomes' morphology was visualized using TEM and all the formulas were discovered to possess unilamellar and spherical vesicles. Figure 2 shows the transmission electron micrographs for E1, E2, and E3.

The entrapment efficiency

Table 4 shows a summary of the Entrapment efficiency (EE) of the ethosomes obtained, which were discovered to range from 97.10% to 97.93%., with E1 having the least EE value, followed by E2, and E3.

Evaluation of andrographolide-loaded ethosomal gel

Table 5 shows a summary of the evaluation of the gels, which discovered that all the ethosomal gel colors were white, while the nonethosomal counterparts were pale white. In addition, all the formulas appeared homogenous when spread on a glass slide, and no visible coarse particles were observed. The pH of the ethosomal gels was discovered to fall within the acceptable pH range of the skin (4.5 – 6.5). Also, the ethosomal gels had higher viscosity, compared to the nonethosomal counterparts, due to the presence of phospholipid components in the formulation. Figure 3 illustrates the rheology evaluation which showed all formulas had a thixotropy plastic flow.

In vitro penetration study

Accepted Manuscript

Figure 4 and Table 6 show the skin penetration profile of the andrographolide-loaded ethosomal gels across rat abdominal skin after over 24 hours. According to the results, the cumulative andrographolide penetration for EG1, EG2, EG3, and NEG were 118.90 ± 3.29 μg/cm^2, 129.25 ± 4.66 μg/cm^2, 86. 16 ± 8.22 μg/cm^2, and 40.08 ± 0.90 μg/cm^2, respectively. Table 6 also shows the rates of permeation expressed as the flux value at steady state of andrographolide ethosomal gels were higher, compared to the nonethosomal counterparts. EG2 had the highest cumulative and flux of andrographolide penetration into the skin, compared to the other gels. Based on Table 6, the lag time of andrographolide for EG1, EG2, EG3, and NEG were 27.59 ± 6.65 min, 3.75 ± 3.07 min, 52.49 ± 5.51 min, and 73.38 ± 12.54 min, respectively. Also, the andrographolide penetration from all ethosomal gels had a shorter lag time, compared to the nonethosomal counterparts.

Stability study

Figures 5 and 6 show the stability studies of the ethosomes, where an increase in the particle size and polydispersity index was observed during 3 months of storage. The particle size of E1, E2, and E3 after 3 months ranged from 145.00 to 210.67 nm, 274.33 to 286.67 nm, and 386.33 to 647.33 nm at storage temperatures of 5°C, 30°C, and 40°C, respectively.

Stability studies were also carried out to evaluate the physical and chemical properties of the ethosomal and nonethosomal gels. The results showed the physical appearance of all gel formulations stored at 5°C did not change during storage for 3 months. However, yellowish-white discoloration was observed in the ethosomal gel stored at 30°C and 40°C. Higher temperature also led to the conversion of the constituent phospholipid into liquid state, consequently, reducing the ethosomal gels' viscosities.

Figure 7 shows the stability profile of ethosomal and non-ethosomal gel, in terms of pH, where the pH of all formulations was discovered to decrease during storage for months.

Accepted Manuscript

After 3 months of storage, the pH value of EG1, EG2, EG3 dan NEG at 30 ± 2°C were discovered to be 4.85, 4.72, 4.69, and 6.17, respectively. However, these pH values are also in the acceptable range of the skin's pH balance.

In addition, the andrographolide content of all the gels decreased during storage for 3 months, however, the new values obtained met the specification (90-110%). According to Figure 8, gel preparations stored at 40°C undergo higher decomposition and, therefore, experience a greater reduction in andrographolide content. In this study, the andrographolide content of EG1, EG2, EG3, and NEG, ranged from 98.13 to 104.19%, 97.93 to 104.01%, and 97.23 to 102.26%, after storage for 3 months at 5 °C, 30 °C, and 40, respectively.

Discussion

Vesicle size plays a crucial role in transdermal drug delivery. Table 3 shows the vesicle size measurements obtained using dynamic light scattering method, which were below 300 nm for all the andrographolide-loaded ethosomes, with E1 having the least vesicle size, followed by E2 and E3. Based on these results, the vesicle size increased with an increase in the phospholipid content, and this is probably due to the enhancement of the vesicle membrane's thickness. A study by Pathan *et al*.,[16] reported an increase in the vesicle size of curcumin-loaded ethosomes, with an increase in the soybean lecithin content. Similarly, Chourasia *et al*.,[21] discovered the soy phosphatidylcholine concentration had a linear relationship with the vesicle size of ketoprofen ethosome.

The determination of vesicle size using DLS also generates the polydispersity index (PDI) value, which shows the degree of heterogeneity in a dispersed system based on particle sizes. A low PDI value (< 0.5) implies the particle in suspension are more homogeneously dispersed.[22] Table 3 shows the PDI of all the ethosome formulas were below 0.3, indicating homogeneous size distribution of vesicles.

Accepted Manuscript

Using the same tool, the value of zeta potential was also determined in triplicate. Particles with higher zeta potential have greater electrical repulsion which avoids particle aggregation, leading to a disperse system with good stability.[23] The zeta potentials of the ethosomes obtained were close to or above -30 mV, with E2 having the highest value of -39.3 ± 0.82 mV. These zeta potential values indicate a disperse system with good stability, and show E2 is the most stable formula. The ethosomes produced had negative zeta potential triggered by the pH value of the hydration medium. Phosphatidylcholine is a zwitterion with an isoelectric point of pH 6-7, which acquired a negative charge due to the use of phosphate pH 7.4 buffer. Furthermore, ethanol imparts a negative surface charge which prevents vesicle aggregation.[16,22] This was proven in the study by Touitou *et al*.,[14] where liposome containing 2% of phospholipid and no ethanol was observed to possess a positive zeta potential. However, the incorporation of ethanol into vesicle formulation induced a transition from positive to negative charge. Similarly, Jain *et al*.,[24] discovered an increase in ethanol content produced more negative zeta potential in diclofenac-loaded ethosomes.

The surface charge of lipid vesicle influences drug permeation across the skin. Negatively charged vesicles tend to demonstrate a higher penetration rate through the skin, compared to their positively charged counterparts, leading to increased drug accumulation.[25] A study by Gillet *et al*.,[26] showed the presence of a negative charge in a vesicle significantly enhances percutaneous permeation of betamethasone and betamethasone dipropionate, compared to ethanolic solution, neutral and positively charged liposome.

Figure 2 shows the evaluation of vesicle morphology using TEM, where the ethosomes were discovered to possess unilamellar and spherical shapes. Spherical-shaped vesicles are formed in cases where phospholipids are hydrated within an aqueous medium and undergo self-assembly into a closed bilayer structure entrapping the aqueous phase within. The hydrophilic

Accepted Manuscript

groups of phospholipids are oriented toward the interior and exterior aqueous phases.[27] Furthermore, the TEM image also confirmed the particle size which was initially observed with the dynamic light scattering method. According to Figure 2, the vesicle size was followed the DLS results' findings, which showed E1 was below 100 nm, while E2 and E3 were above 100 nm.

Table 4 shows the EE values of all the ethosomes produced were above 97%, with the highest value recorded for E3 which contained the highest phospholipid concentration. An increase in the phospholipid content tends to increase vesicle membrane's size and strength, consequently, increasing the amount of entrapped drugs.[16,21] Andrographolide is a lipophilic drug entrapped primarily in the lipid bilayer of the vesicle, therefore, an increase in the phospholipid improves the entrapment efficiency. Shen *et al*.,[28] reported an increase in the entrapment efficiency of apigenin ethosome with an increase in the concentration of soybean lecithin. An increase in the phospholipid content increases the volume of vesicular space and consequently, tends to improve the drug entrapment. This was proven in a study by Chourasia *et al*.,[21] where a positive relationship was discovered between the concentration of soybean phosphatidylcholine and the entrapment of ketoprofen inside the ethosome.

In this study, the ethosomes obtained were incorporated into gel preparations to make the system more suitable for transdermal application, using HPMC as a gelling agent. HPMC is a nonionic, non-irritating, synthetic polymer, which is stable in a wide pH range (3-11), generally recognized as safe (GRAS-listed), and consequently, widely used in topical formulations.[29] Also, the viscosity of a gel preparation is important to facilitate application on the skin more easily and control the release profile of drugs.[30]

The *in vitro* penetration study of andrographolide ethosomal gels was conducted for 24 hours with 18 sampling time points. The results showed the least cumulative andrographolide

Accepted Manuscript

penetration was recorded for NEG, followed by EG3, EG1, and EG2. All the ethosomal gels were discovered to possess significantly higher cumulative andrographolide penetration, compared to the nonethosomal counterparts ($P < 0.05$). Table 6 shows the highest flux was recorded for EG2. The rate of drug penetration is probably due to the advantageous combination of the entrapment efficiency, as well as the vesicle size, which is inversely related to the skin permeation of the drug. Vesicles size ≤ 300 nm can penetrate the stratum corneum into the deeper layer of the skin, while vesicles ≥ 600 nm remain in the stratum corneum.[31] The ethosomes developed in this study had vesicles below 300 nm, and were, therefore, able to penetrate easily through the skin and generate higher transdermal flux.[32,33] EG2 had the highest cumulative andrographolide penetrated and flux, most likely because the vesicle size was smaller, compared to E3, while the entrapment efficiency was higher, compared to E1. Among the 3 ethosomal gel preparations, EG3 had the lowest flux because E3 had the biggest vesicle size and, therefore, had the slowest skin penetration rate. Also, the presence of ethanol in the ethosomal gels increased the transdermal flux by about 2-3 folds, compared to the nonethosomal counterparts.

Andrographolide takes time to penetrate across rat skin and diffuse into the receptor compartment until a steady-state condition is attained, as indicated by the lag time parameter. The results showed the ethosomal gel had a shorter lag time, compared to the NEG, indicating the ethosomes reduce the time required to reach steady-state for penetration of andrographolide across the rat skin. This is probably due to the presence of phospholipid, as well as ethanol which enhanced the flexibility of vesicle membrane. The high concentration of ethanol also disordered the lipid domain structure of the stratum corneum and increased the skin permeability.[22] Subsequently, the andrographolide was encapsulated in phospholipid vesicles which had a similar coefficient partition with the lipid of stratum corneum. These properties allow ethosomes to easily deliver andrographolide through the skin.[19] Table 6

Accepted Manuscript

shows EG2 had the shortest lag time, compared to EG1, as well as EG3, and this is probably due to the rapid diffusion of EG2 which had a smaller vesicle size, compared to EG3 and higher phospholipid content, compared to EG1, consequently, enabling easy penetration.

Based on the results of *in vitro* penetration study, the andrographolide-loaded ethosomes developed in this study were concluded to enhance andrographolide penetration through the skin. This proves encapsulation into the ethosome improves the transdermal delivery of drugs. Several studies have also reported similar findings, for instance, Yan *et al*.,[34] reported increased sinomenine deposition and permeation using ethosomes. A separate study also reported a higher cumulative penetration and flux with indomethacine ethosome, compared to other formulations.[35]

There are several mechanisms by which ethosome could increase the delivery of drugs across the skin. A combination of phospholipid and ethanol component in the ethosomes has been suggested to increase skin penetration and distribution.[36] The ethanol content in the ethosome is bound to fluidize and decrease the structural density of the lipid bilayer which reduces the stratum corneum's barrier property. Ethanol also interacts with the hydrophilic head group of a phospholipid, consequently, generating a more flexible vesicle structure that penetrates more easily through the stratum corneum's disorganized lipid bilayer. These effects increase the percutaneous permeation of the drug.[37]

The stability of the ethosomes developed was studied for 3 months and the vesicle sizes of ethosomes stored at 5°C and 30°C were discovered to tend to increase during storage but remained below 300 nm. This showed the ethosomes retained their ability to permeate into the deeper layer of the skin and the increase in vesicle sizes was suggested to be due to vesicle aggregation. The polydispersity index of ethosomes was found to increase after

Accepted Manuscript

storage for 3 months, however, the values remained below 0.5, indicating all ethosomes retained their homogeneous size distribution.

Furthermore, the pH of the andrographolide ethosomal and nonethosomal gels were discovered to reduce during storage for 3 months at 5°C, 30°C, and 40°C, due to the hydrolysis of phosphatidylcholine. In an aqueous medium, phosphatidylcholines undergo hydrolysis to generate lysophospholipid and fatty acid, which provides free proton, leading to a reduction in pH.[38] Based on the stability results, EG3 had the lowest pH, compared to EG1, as well as EG2, and this is because EG3 had the highest amount of phospholipid content. The hydrolysis rate of phospholipid is temperature dependent, thus, an elevation in temperature increases the hydrolysis rate and produces more fatty acid.[39] Therefore, the ethosomal gels stored at 30°C and 40°C, had lower pH, compared to the counterparts stored at low temperature.

The andrographolide content of the gels was reduced after 3 months of storage. However, this is in line with the specification of the andrographolide content (90 to 110%). Andrographolide containing ester-linked hydrocarbon chain is susceptible to hydrolysis in aqueous dispersion. This chemical reaction degrades andrographolide by opening the lactone ring structure and forming deoxyandrographolide, leading to a reduction in the andrographolide content. At higher temperatures, andrographolide is less stable,[39,40] therefore, greater reductions in the andrographolide content were observed at 30°C and 40°C.

Conclusion

This study successfully developed andrographolide-loaded ethosomes using the thin layer hydration method. The 3 ethosome formulas had vesicle sizes below 300 nm, polydispersity index below 0.3, good zeta potential, and high entrapment efficiency, with EG2 having the highest cumulative andrographolide penetration, as well as the highest penetration flux

Accepted Manuscript

through the skin. Therefore, ethosomal gel is a potentially useful carrier for increasing andrographolide skin penetration.

Acknowledgment

The authors are grateful to the Universitas Indonesia for the provision of financial aid towards this study through the PUTI Saintekes Research Grant 2020, under contract number NKB-2090/UN2.RST/HKP.05.00/2020.

Ethical Clearance

The *in vitro* skin penetration study using male *Sprague-Dawley* rats was approved by the Ethical Clearance Committee of Faculty of Medicine, Universitas Indonesia (No. KET-255/UN2.F1/ETIK/PPM.00.02/2020).

Author Contributions

NM contributed to the study conception, design, literature search, data acquisition, data analysis, manuscript preparation, and editing. Meanwhile, SS contributed to the study conception, supervising the work, data analysis, manuscript editing, and reviewing and AB contributed to the data analysis and manuscript review.

Conflicts of interest

The authors declare no conflicts of interest.

References

1. Pawar A, Rajalakshmi S, Mehta P, Shaikh P, Bothiraja C. Strategies for formulation development of andrographolide. *RSC Adv* 2016;6:69282-69300. doi: 10.1039/C6RA12161F.

Accepted Manuscript

2. Tan WSD, Liao W, Zhou S, Wong WSF. Is there a future for andrographolide to be an anti-inflammatory drug? Deciphering its major mechanisms of action. *Biochem Pharmacol* 2017;139:71–81. doi: 10.1016/j.bcp.2017.03.024.
3. Burgos RA, Hancke JL, Bertoglio JC, Aguirre V, Arriagada S, Calvo M, et al. Efficacy of an Andrographis paniculata composition for the relief of rheumatoid arthritis symptoms: a prospective randomized placebo-controlled trial. *Clin Rheumatol* 2009;28:931–946. doi: 10.1007/s10067-009-1180-5.
4. Li Z, Tan J, Wang L, Li Q. Andrographolide benefits rheumatoid arthritis via inhibiting MAPK pathways. *Inflammation* 2017; doi: 10.1007/s10753-017-0600-y.
5. Yan J, Chen Y, He C, Yang ZZ, Lu C, Chen XS. Andrographolide induces cell cycle arrest and apoptosis in human rheumatoid arthritis fibroblast-like synoviocytes. *Cell Biol Toxicol* 2012;28(1):47-56. doi: 10.1007/s10565-011-9204-8.
6. Chen H-W, Huang C, Li CC, Lin AH, Huang YJ, Wang TS, et al. Bioavailability of andrographolide and protection against carbon tetrachloride-induced oxidative damage in rats. *Toxicol Appl Pharmacol* 2014;280:1–9. doi: 10.1016/j.taap.2014.07.024.
7. Ye L, Wang T, Tang L, Liu W, Yang Z, Zhou J, et al. Poor oral bioavailability of a promising anticancer agent andrographolide is due to extensive metabolism and efflux by p-glycoprotein. *J Pharm Sci* 2011;100:5007–5017. doi: 10.1002/jps.22693.
8. Bothiraja C, Shinde MB, Rajalaksmi S, Pawar AP. Evaluation of molecular pharmaceutical and in-vivo properties of spray-dried isolated andrographolide–PVP. *Journal of Pharmacy and Pharmacology* 2009;61:1465–1472.doi: 10.1211/jpp/61.11.0005.
9. Zhou X, Hao Y, Yuan L, Pradhan S, Shrestha K, Pradhan O, et al. Nano-formulations for transdermal drug delivery: A review. *Chinese Chemical* Letters 2018;29:1713–1724. doi: 10.1016/j.cclet.2018.10.037.

Accepted Manuscript

10. Xie J, Ji Y, Xue W, Ma D, Hu Y. Hyaluronic acid-containing ethosomes as a potential carrier for transdermal drug delivery. *Colloids Surf B Biointerfaces* 2018;172:323–32. doi: 10.1016/j.colsurfb.2018.08.061.
11. Alexander A, Dwivedi S, Ajazuddin, Giri TK, Saraf S, Saraf S, et al. Approaches for breaking the barriers of drug permeation through transdermal drug delivery. *J Control Release* 2012;164:26–40. doi: 10.1016/j.jconrel.2012.09.017.
12. Jain S, Patel N, Shah MK, Khatri P, Vora N. Recent advances in lipid-based vesicles and particulate carriers for topical and transdermal application. *J Pharl Sci* 2016; 2017; 106 (2): 423-445. doi: 10.1016/j.xphs.2016.10.001.
13. Verma P, Pathak K. Therapeutic and cosmeceutical potential of ethosomes: An overview. *J Adv Pharm Technol Res* 2010;1(3):274-82. doi: 10.4103/0110-5558.72415.
14. Touitou E, Dayan N, Bergelson S, Godin B, Eliaz M. Ethosomes — novel vesicular carriers for enhanced delivery: characterization and skin penetration properties. *J Control Release* 2000;65:403–418.
15. Elsayed MMA, Abdallah OY, Naggar VF, Khalafallah NM. Deformable liposomes and ethosomes: Mechanism of enhanced skin delivery. *Int J Pharm* 2006;322:60–66. doi: 10.1016/j.ijpharm.2006.05.027.
16. Pathan IB, Jaware BP, Shelke S, Ambekar W. Curcumin loaded ethosomes for transdermal application: Formulation, optimization, in-vitro and in-vivo study. *Journal of Drug Delivery Science and Technology* 2018;44:49–57. doi: 10.1016/j.jddst.2017.11.005
17. Sasongko RA, Surini S, Saputri FC. Formulation and Characterization of Bitter Melon Extract(*Momordica charantia*) Loaded Phytosomes. *Pharmacogn J*. 2019; 11(6):1235-1241. doi:10.5530/pj.2019.11.192.

Accepted Manuscript

18. Ahad A, Raish M, Al-Mohizea AM, Al-Jenoobi FI, Alam MA. Enhanced anti-inflammatory activity of carbopol loaded meloxicam nanoethosomes gel. *Int J Biol Macromol* 2014;67:99–104. doi: 10.1016/j.ijbiomac.2014.03.011.

19. Surini S, Arnedy AR, Iswandana R. Development of Ethosome Containing Bitter Melon (Momordica charantia Linn.) Fruit Fraction and In Vitro Skin Penetration. *Pharmacogn J*. 2019; 11(6):1242-1251. doi:10.5530/pj.2019.11.193.

20. Suo XB, Zhang H, Wang YQ. HPLC determination of andrographolide in rat whole blood: study on the pharmacokinetics of andrographolide incorporated in liposomes and tablets. *Biomed. Chromatogr* ;2007:21:730–734. doi: 10.1002/bmc.812.

21. Chourasia MK, Kang L, Chan SY. Nanosized ethosomes bearing ketoprofen for improved transdermal delivery. *Results in Pharma Sciences* 201;1:60–67. doi:10.1016/j.rinphs.2011.10.002.

22. El-Alim SHA, Kassem AA, Basha M, Salama A. Comparative study of liposomes, ethosomes and transfersomes as carriers for enhancing the transdermal delivery of diflunisal: In vitro and in vivo evaluation. *Int J Pharm* 2019;563:293–303. Doi: 10.1016/j.ijpharm.2019.04.001.

23. Malvern. Zetasizer nano series user manual. Worcestershire: Malvern Instruments Ltd; 2013.

24. Jain S, Patel N, Madan P, Lin S. Quality by design approach for formulation, evaluation and statistical optimization of diclofenac-loaded ethosomes via transdermal route. Pharm Dev Technol 2014; Early Online:1–18.

25. Sinico C, Manconi M, Peppi M, Lai F, Valenti D,Fadda AM. Liposomes as carriers for dermal delivery of tretinoin: in vitro evaluation of drug permeation and vesicle–skin interaction. *J Control Release* 2005;103:123–136. doi:10.1016/j.jconrel.2004.11.020.

Accepted Manuscript

26. Gillet A, Compere P, Lecomte F, Hubert P,Ducat E, Evrard B,et al. Liposome surface charge influence on skin penetration behaviour. *Int J Pharm* 2011;411:223–231. doi:10.1016/j.ijpharm.2011.03.049.

27. Akbarzadeh A, Sadabady RR, Davaran S, Joo SW, Zarghami N, Hanifehpour Y, et al. Liposome: classification, preparation, and Applications. *Nanoscale Research Letters* 2013;8:102.

28. Shen LN, Zhang YT, Wang Q, Xu L, Feng NP. Enhanced in vitro and in vivo skin deposition of apigenin delivered using ethosomes. *Int J Pharm* 2014;460:280– 288.

29. Vlaia L, Coneac G, Olariu I, Vlaia V, Lupuleasa D. Emerging concepts in analysis and applications of hydrogelscellulose-derivatives-based hydrogels as vehicles for dermal and transdermal drug delivery. *Intech* 2016. doi: 10.5772/63953.

30. Oktay AN, Tamer SI, Han S, Uludag O, Celebi N. Preparation and in vitro / in vivo evaluation of flurbiprofen nanosuspension based gel for dermal application. *European Journal of Pharmaceutical Sciences* 2020;155:105548. doi: 10.1016/j.ejps.2020.105548.

31. Verma DD, Verma S, Blume G, Fahr A. Particle size of liposomes influences dermal delivery of substances into skin. *Int J Pharm* 2003;258:141–151. doi:10.1016/S0378-5173(03)00183-2.

32. Maestrelli F, Capasso G, Rodriguez M, Rabasco AM, Ghelardini C, Mura, P. Effect of preparation technique on the properties and in vivo efficacy of benzocaine-loaded ethosomes. *J Liposome Res* ;2009:19(4): 253–260.

33. Hua S. Lipid-based nano delivery systems for skin delivery of drugs and bioactives. *Front Pharmacol* 2015;6:219. doi: 10.3389/fphar.2015.00219.

34. Yan Y, Zhang H, Sun J, Wang P, Dong K, Dong Y, et al. Enhanced transdermal delivery of sinomenine hydrochloride by ethosomes for anti-inflammatory treatment. *Journal of*

Accepted Manuscript

Drug Delivery Science and Technology 2016;36:201-207. doi: 10.1016/j.jddst.2016.10.013.

35. Sakdiset P, Amnuaikit T, Pichayakorn W, Pinsuwan S. Formulation development of ethosomes containing indomethacin for transdermal delivery. *Journal of Drug Delivery Science and Technology* 2019;52:760–768.
36. Touitou E, Godin B, Dayan N, Weiss C, Piliponsky A, Schaffer FL. Intracellular delivery mediated by an ethosomal carrier. *Biomaterials* 2001;22:3053–3059.
37. Bodade SS, Shaikh KS, Kamble MS, Chaudhary PD. A study on ethosomes as mode for transdermal delivery of an antidiabetic drug. *Drug Deliv* 2013;20(1):40–46. Doi: 10.1016/s0142-9612(01)00052-7.
38. Grit M, Crommelin DJA. Chemical stability of liposomess: implications for their physical stability. *Chem Phys Lipids* 1993;64:3-18.
39. Rafi M, Devi AF, Syafitri UD, Heryanto R, Suparto IH, Amran MB, et al. Classification of Andrographis paniculata extracts by solvent extraction using HPLC fingerprint and chemometric analysis. *BMC Res Notes* 2020;13:56. doi: 10.1186/s13104-020-4920-x
40. Yan Y, Fang LH, Du GH. Andrographolide. In: Du GH. Natural small molecule drugs from plants:. Springer Nature Singapore Pte Ltd. and People's Medical Publishing House; 2018. p. 357-62.

Accepted Manuscript

Tables

Table 1: The formulation of andrographolide-loaded ethosomes.

Material	E1	E2	E3
Andrographolide (g)	0.5	0.5	0.5
Phospholipon 90 G (g)	4.0	4.5	5.0
Ethanol (mL)	6.0	6.0	6.0
Propylene glycol (mL)	1.5	1.5	1.5
Phosphate buffer pH 7,4 (mL)	22.5	22.5	22.5

E1: ethosome formula 1; E2: ethosome formula 2; E3: ethosome formula 3

Table 2: Formulation andrographolide-loaded ethosomal gel

Material	Formula (% w/w)			
	EG1	EG2	EG3	NEG
Andrographolide loaded ethosome	Equal to 1 gram andrographolide	Equal to 1 gram andrographolide	Equal to 1 gram andrographolide	-
Andrographolide	-	-	-	1
HPMC	1.5	1.5	1.5	1.5
Propylene glycol	5	5	5	5
Methylparaben	0.06	0.06	0.06	0.06
Propylparaben	0.03	0.03	0.03	0.03
Demineralized water	Ad 100	Ad 100	Ad 100	Ad 100

EG: andrographolide-loaded ethosomal gel, NEG: andrographolide-loaded nonethosomal gel

Accepted Manuscript

Table 3: Characteristics of the andrographolide-loaded ethosomes

Formula	Dv_{90} (nm)	Z-Average (nm)	Polydispersity Index	Zeta Potential (mV)
E1	92.27 ± 5.23	87.40 ± 0.54	0.253 ± 0.008	-29.67 ± 1.03
E2	107.10 ± 11.25	89.95 ± 0.75	0.254 ± 0.020	-39.30 ± 0.82
E3	123.00 ± 11.36	100.25 ± 2.06	0.275 ± 0.011	-33.43 ± 0.97

All values are represented as mean ± SD.

Table 4: The entrapment efficiency of andrographolide-loaded ethosomes

Formula	Entrapment Efficiency (%)
E1	97.10 ± 0.05
E2	97.89 ± 0.02
E3	97.93 ± 0.00

All values are represented as mean ± SD.

Table 5: Evaluation of andrographolide-loaded ethosomal and nonethosomal gel.

Parameter	EG1	EG2	EG3	NEG
Organoleptic	White, homogeneous	White, homogeneous	White, homogeneous	Pale white, homogeneous
pH	6.01	6.06	6.02	7.37
Viscosity	62878 cPs	64357 cPs	68496 cPs	49889 cPs
Rheology	Thixotropy plastic flow	Thixotropy plastic flow	Thixotropy plastic flow	Thixotropy plastic flow

Accepted Manuscript

Table 6: The cumulative andrographolide penetration, *in vitro* flux, lag time, and enhancement ratios of ethosomal and nonethosomal gel.

Formula	Cumulative amount of andrographolide ($\mu g/cm^2$)	Flux ($\mu g/cm^2$/hour)	Lag Time (minutes)	Enhancement Ratio
EG1	118.90 ± 3.29	4.74 ± 0.07	27.59 ± 6.65	2.68
EG2	129.25 ± 4.66	5.16 ± 0.10	3.75 ± 3.07	2.92
EG3	86. 16 ± 8.22	3.66 ± 0.27	52.49 ± 5.51	2.07
NEG	40.08 ± 0.90	1.77 ± 0.03	73.38 ± 12.54	1.00

All values are represented as mean ± SD.

Accepted Manuscript

List of Figures

Figure 1: The Particle size distribution of andrographolide-loaded ethosome. (a) E1; (b) E2; and (c) E3.

Figure 2: Morphology of andrographolide-loaded ethosome. (a) E1, x100 000 magnification; (b) E2, x70 000 magnification; (c) E3, x70 000 magnification.

Figure 3: Rheogram of andrographolide ethosomal and non ethosomal gel.

Figure 4: The cumulative andrographolide penetration from gel preparations.

Figure 5: The particle size of andrographolide ethosome during 3 months at (a) 5 ± 2°C; (b) 30 ± 2°C; and (c) 40 ± 2°C.

Figure 6: The polidispersity index of andrographolide ethosome during 3 months at (a) 5 ± 2°C; (b) 30 ± 2°C; and (c) 40 ± 2°C.

Figure 7: The pH of andrographolide-loaded ethosomal and nonethosomal gel during storage for 3 months at (a) 5 ± 2°C; (b) 30 ± 2°C; and (c) 40 ± 2°C.

Figure 8: The stability profile of andrographolide-loaded ethosomal and nonethosomal gel showing the total drug content (%) during storage for 3 months at (a) 5 ± 2°C; (b) 30 ± 2°C; and (c) 40 ± 2°C.

Accepted Manuscript

Figures

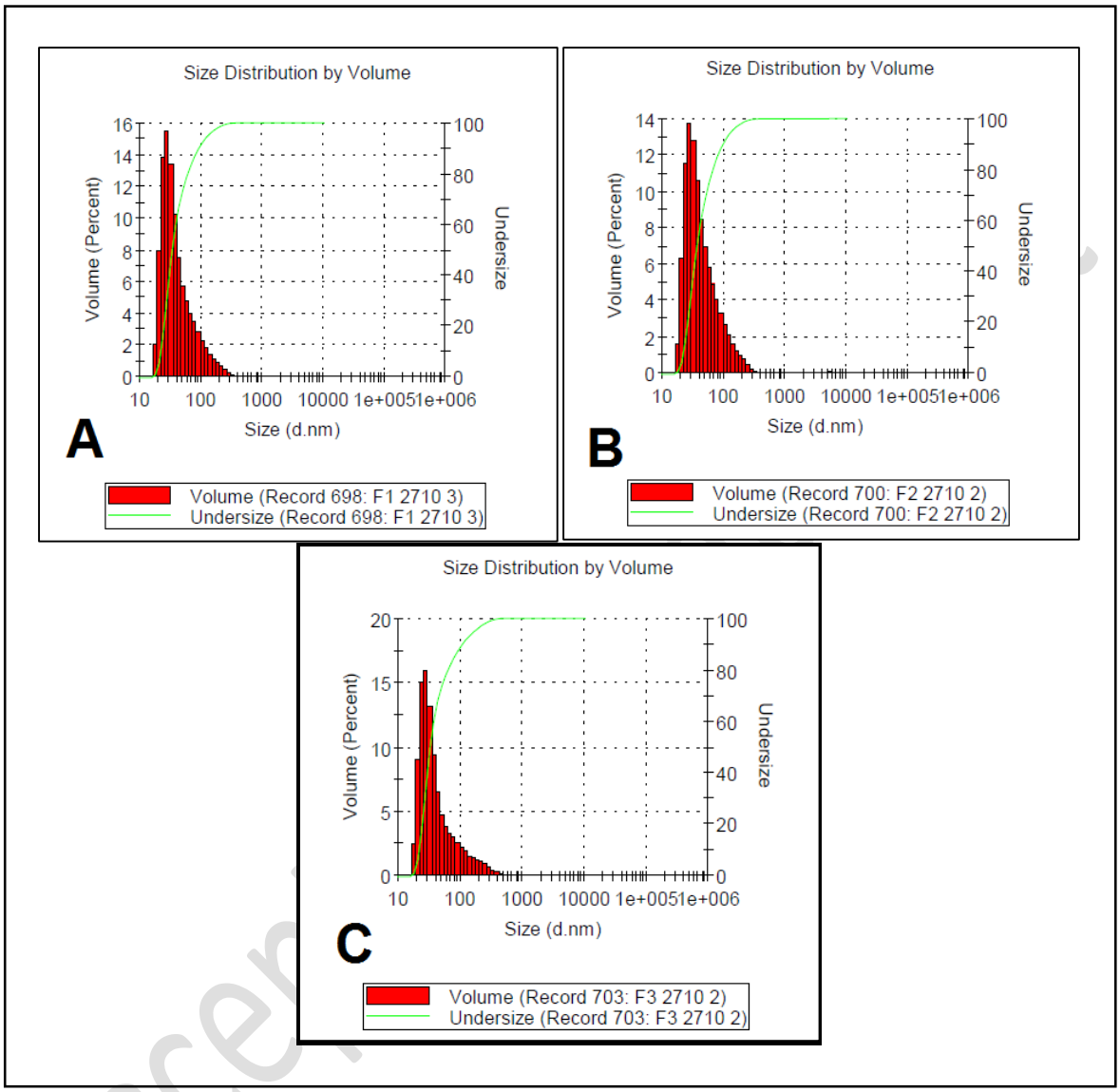

Figure 1: The particle size distribution of andrographolide-loaded ethosome. (a) E1; (b) E2; and (c) E3.

Accepted

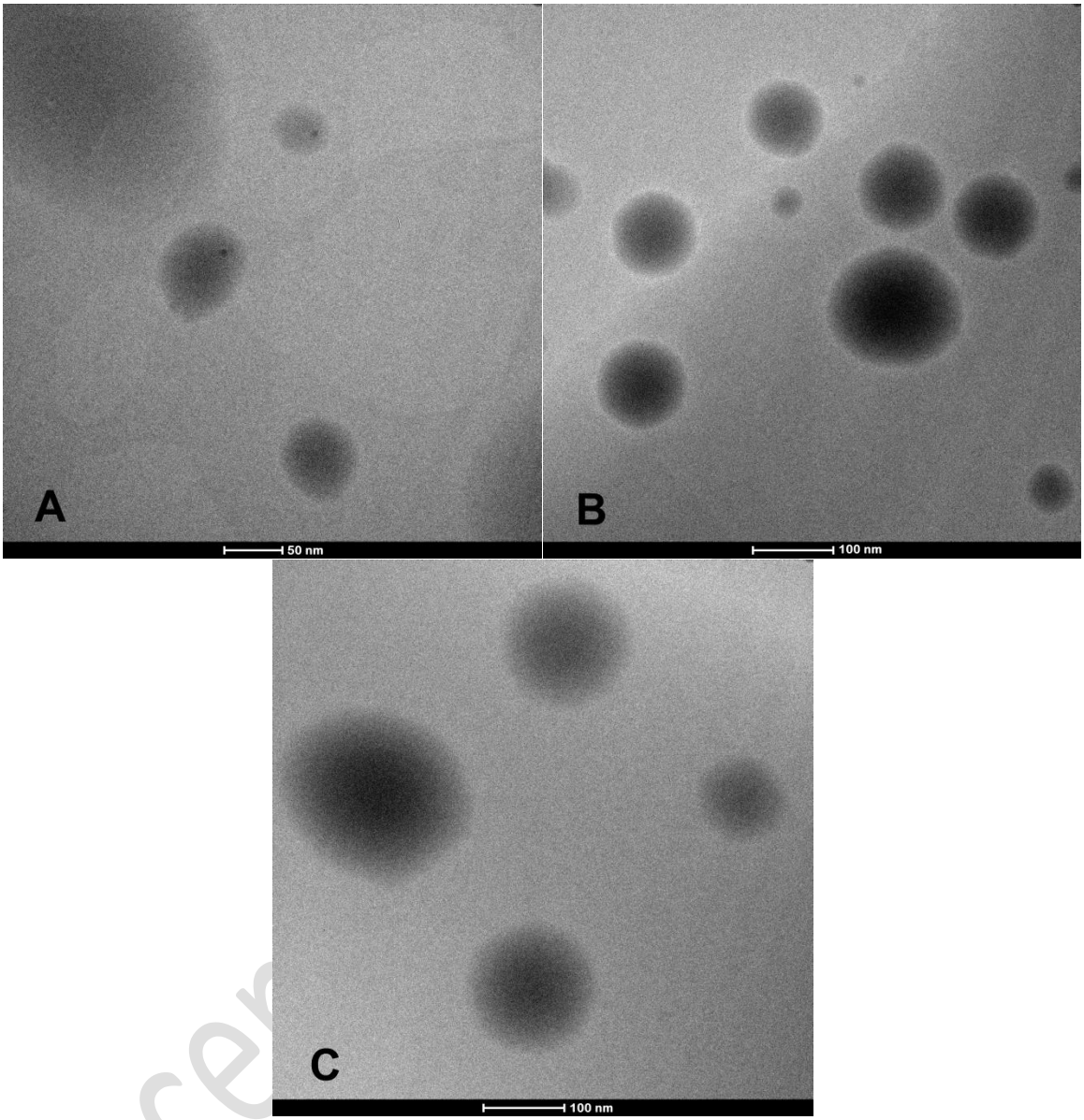

Figure 2: Morphology of andrographolide-loaded ethosome. (a) E1, x100,000 magnification; (b) E2, x70,000 magnification; (c) E3, x70,000 magnification.

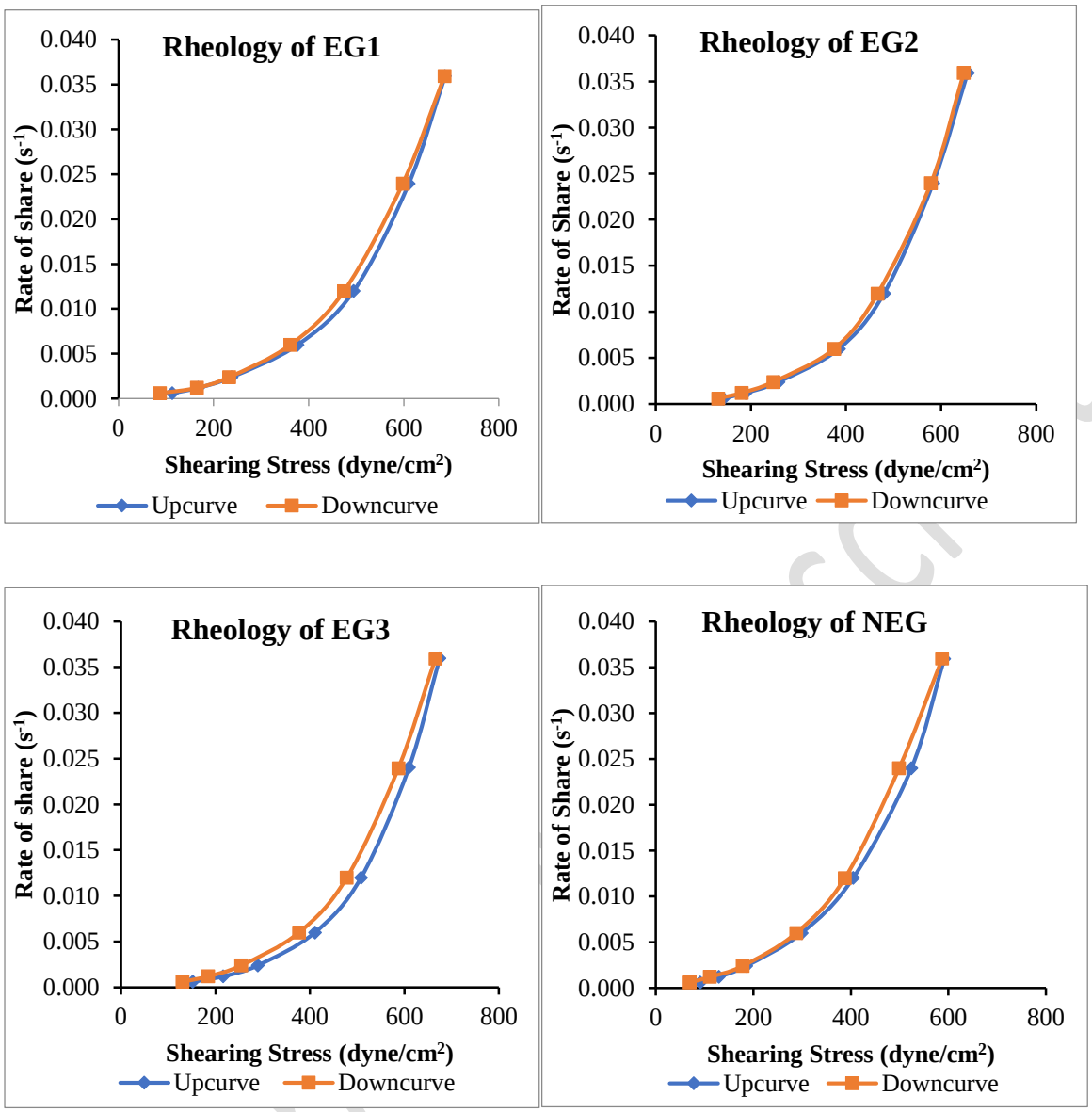

Figure 3: The rheogram of andrographolide ethosomal and nonethosomal gel.

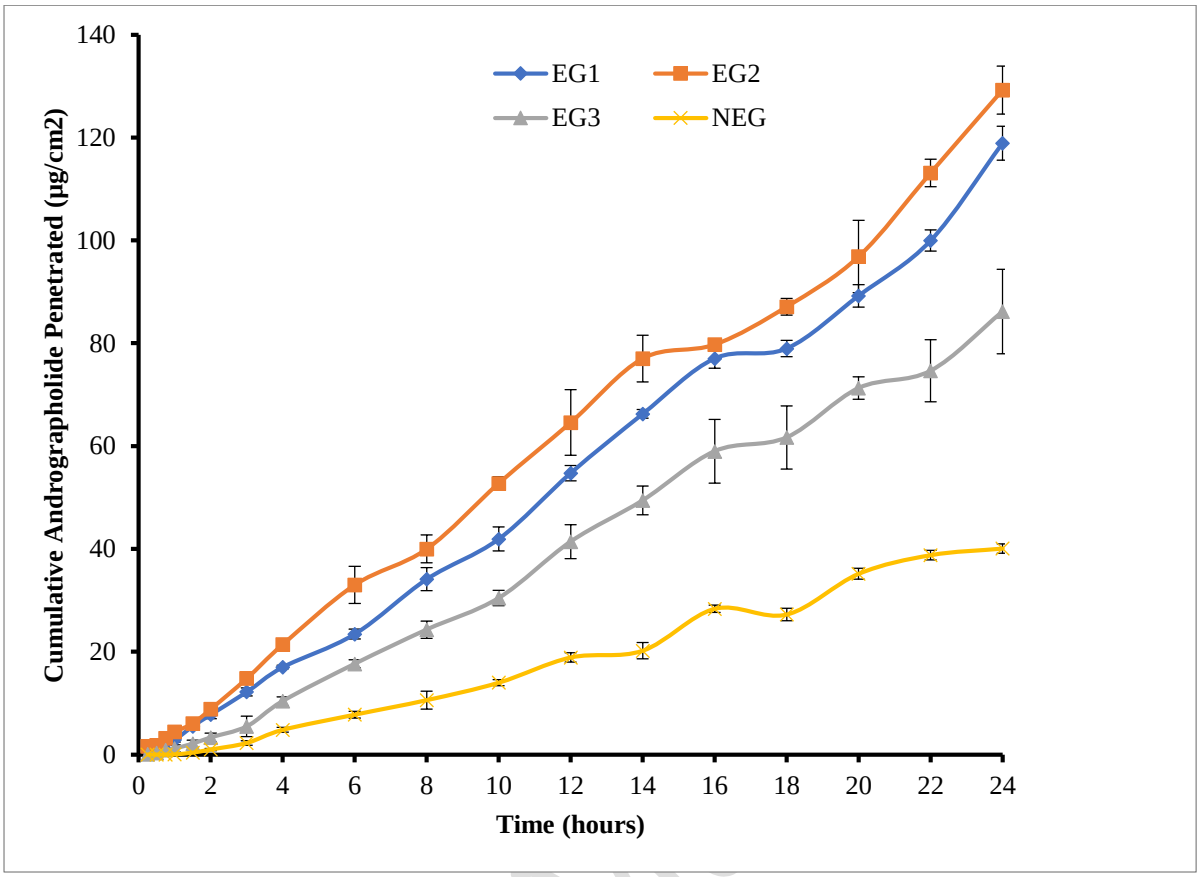

Figure 4: The cumulative andrographolide penetration from the gel preparations.

Accepted Manuscript

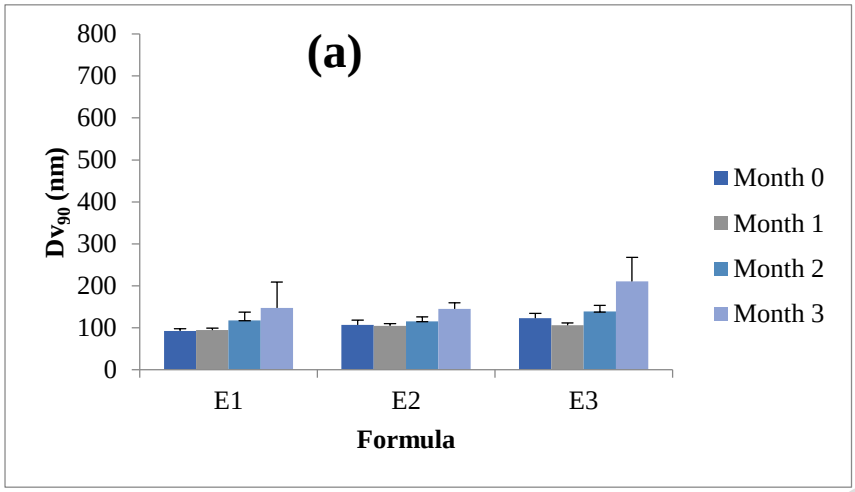
(a)
800
700
600
500
400
300
200
100
0
Dv90 (nm)
E1
E2
E3
Formula
Month 0
Month 1
Month 2
Month 3

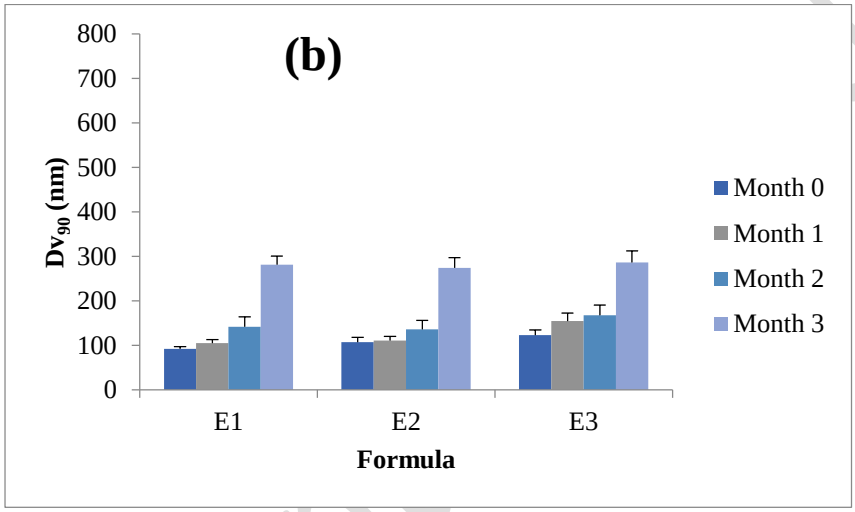
(b)
800
700
600
500
400
300
200
100
0
Dv90 (nm)
E1
E2
E3
Formula
Month 0
Month 1
Month 2
Month 3

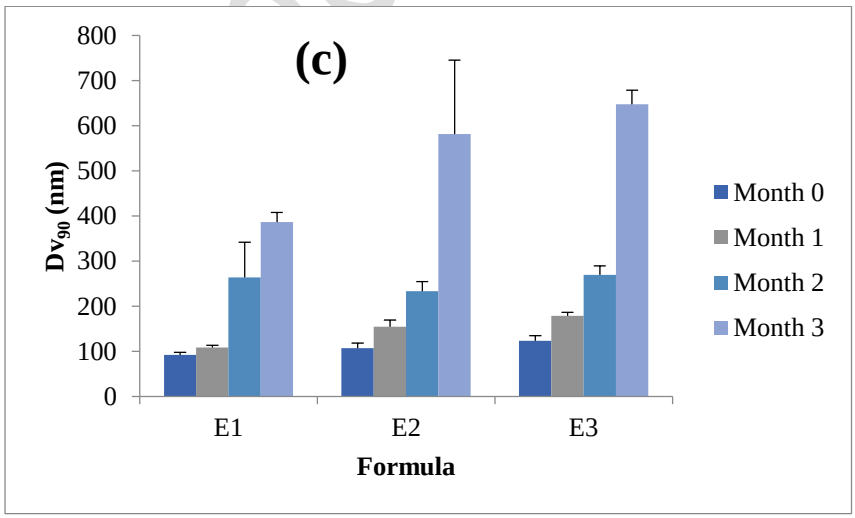
(c)
800
700
600
500
400
300
200
100
0
Dv90 (nm)
E1
E2
E3
Formula
Month 0
Month 1
Month 2
Month 3

Figure 5: The Particle size (Dv_{90}) of andrographolide ethosome during 3 months storage at (a) 5 ± 2°C; (b) 30 ± 2°C; and (c) 40 ± 2°C.

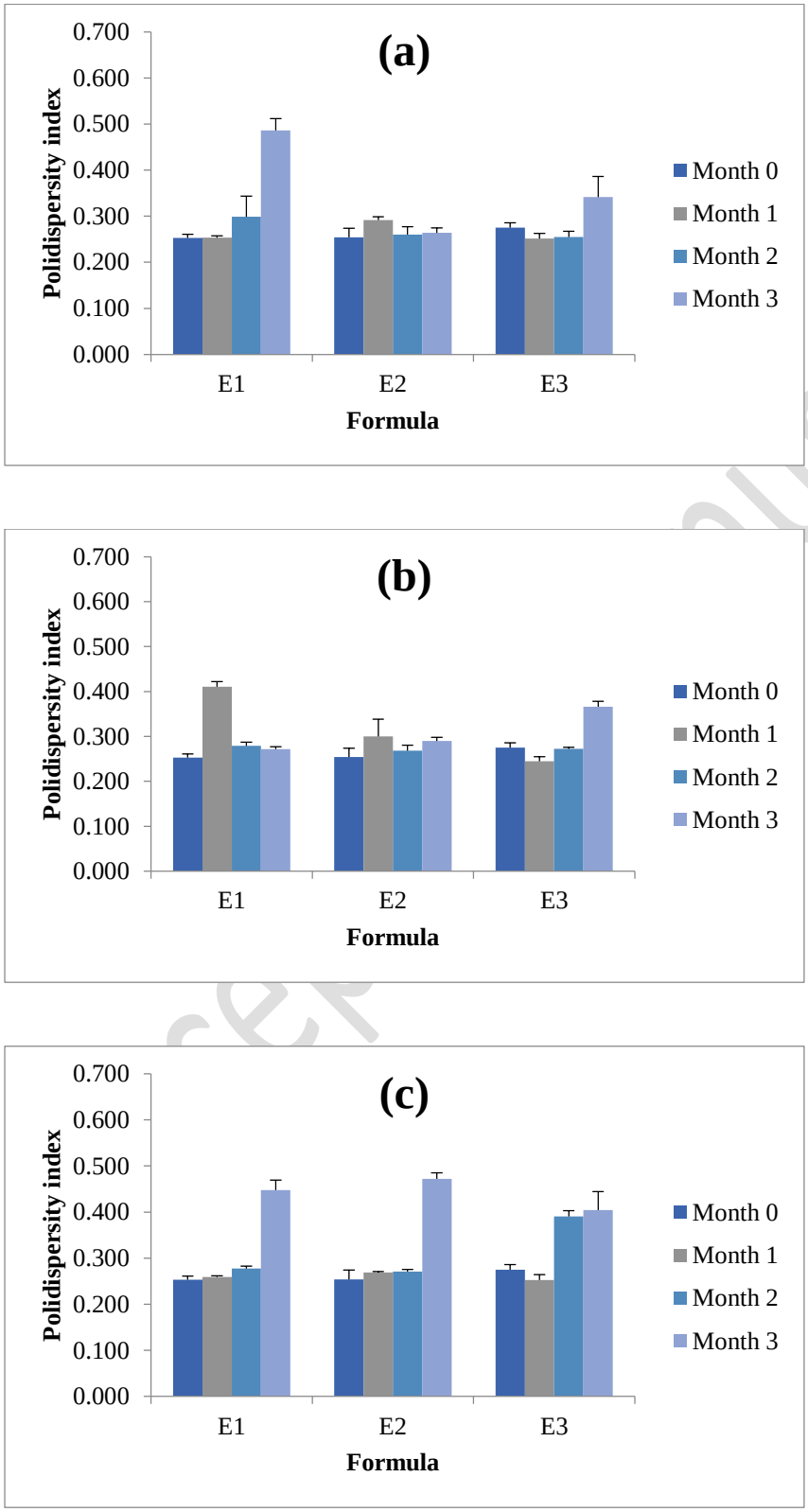

Figure 6: The polidispersity index of andrographolide ethosome during 3 months at (a) 5 ± 2°C; (b) 30 ± 2°C; and (c) 40 ± 2°C.

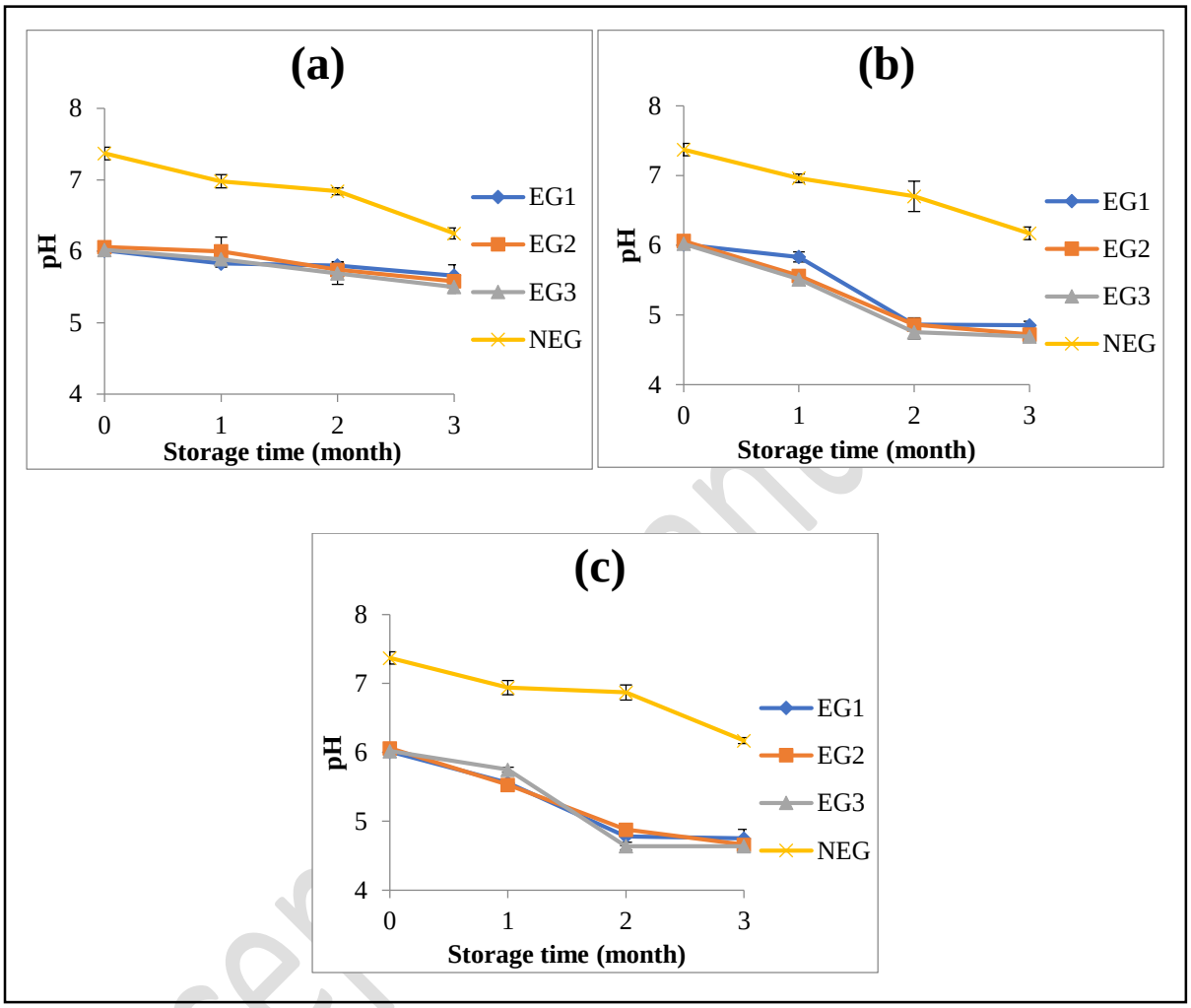

Figure 7: The pH of andrographolide-loaded ethosomal and nonethosomal gel during 3 months storage at (a) 5 ± 2°C; (b) 30 ± 2°C; and (c) 40 ± 2°C.

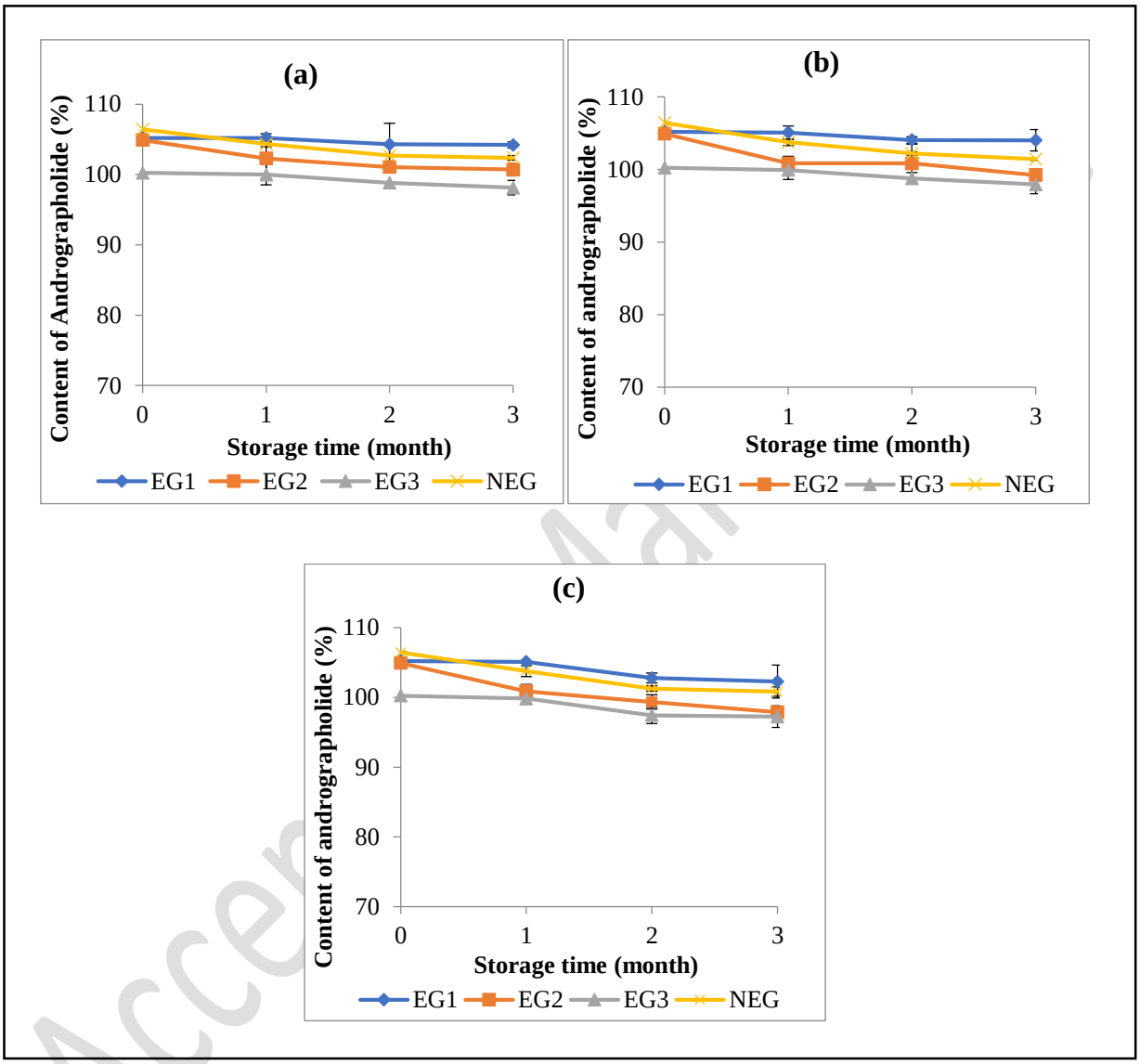

Figure 8: Stability profile of andrographolide-loaded ethosomal and nonethosomal gel showing total drug content (%) during 3 months at (a) 5°C; (b) 30 ± 2°C; and (c) 40 ± 2°C.